

Back-Projection technique for a Slanted Scanning Sky Monitor Camera

Ravi Shankar BT and Dipankar Bhattacharya

May 20, 2004

Abstract

The procedure of the Back-Projection Image Reconstruction for the slanted cameras of the Scanning Sky Monitor (SSM) assembly aboard ASTROSAT, the procedure for generating the Point Spread Functions (PSF) and the Iterative Removal Of Sources (IROS) (the PSF-removal procedure) are described in this report.

Contents

1.1	Simulation	1
1.2	Image Reconstruction: Derotation and Back-Projection	2
1.3	Iterative Removal Of Sources	4
1.3.1	PSF-generation	4
1.3.2	The procedure of IROS	5
1.4	Noise Characteristics	6

1.1 Simulation

The working of the slanted cameras of SSM is simulated using Monte Carlo methods. The mask plate of the camera is assumed to have six mask patterns (of 63 mask elements each) placed one next to the other with an inter-pattern gap of 2 mm and the detector is assumed to consist of eight wires (refer figure 1.1). As shown in the figure, X-direction is along the mask coding direction and Y-direction is across that direction.

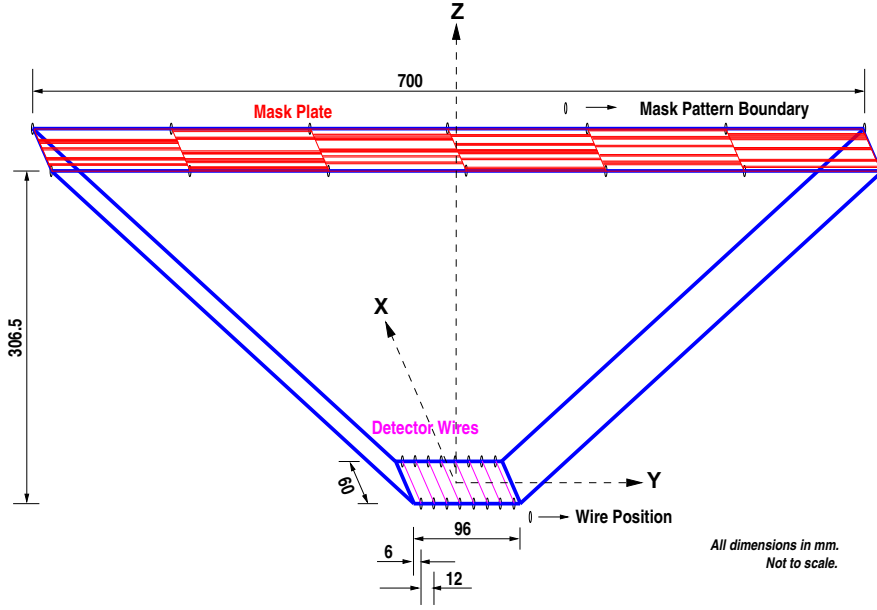


Figure 1.1: The dimensions of the camera

The camera is rotated along the X direction for a chosen *exposure interval* at a specified rate (a value of $\frac{1}{15}^\circ/s$ has been used). The *exposure interval* is selected to be equal to the traversal time of a source through the full camera field of view due to camera rotation and is calculated as:

$$t_e = \frac{2 \times \tan^{-1} \left(\frac{w_x}{h} \right)}{\dot{\theta}_x}$$

where,

- t_e \equiv Total Exposure Time, s
- w_x \equiv Mask Plate Width Along X direction = 60 mm
- h \equiv Distance between the mask plane and the wire plane = 306.5 mm
- $\dot{\theta}_x$ \equiv Rate of Rotation of the camera along X direction, $^\circ/s$
(A value of $\frac{1}{15}^\circ/s$ has been used during simulations).

For a specified value of the flux of the source (in units of Crab), the time interval between the generated photons is calculated as:

$$t_i = \frac{100}{f_c \times f_s \times w_x \times w_y}$$

where,

- t_i \equiv Time interval between generated photons, s
- f_c \equiv Integrated Counts from Crab for SSM over the energy range of 2 keV – 10 keV = 3.58 counts(cts) $\text{cm}^{-2} \text{s}^{-1}$ (from simulations)
- f_s \equiv Specified value of flux of the source to be used during simulation, Crab
- w_y \equiv Mask plate width along Y-direction = 700 mm

The value of the number of photons to be generated for the specified source is then obtained as:

$$n_g = \frac{t_e}{t_i}$$

The rotation is simulated by keeping the camera stationary and shifting the source location (starting with the specified location) in a direction opposite to that of the specified camera rotation. At intervals of t_i s, a photon is made to strike at random locations on the mask plate and if this strike position happens to be in an open mask area, the photon is made to strike the detector at the specified source angle. An event list consisting of the information about the photons striking the detector is generated. For every photon in the event list, the strike-position along the X-direction, the sequential number of the wire in whose cell it is detected and the strike-time are recorded.

1.2 Image Reconstruction: Derotation and Back-Projection

From the recorded event list, a chunk of data corresponding to the exposure time (t_e) is selected and a *fiducial time* is chosen at the middle of the selected data.

$$t_f = t_0 + \frac{t_e}{2}$$

where,

$$\begin{aligned} t_f &\equiv \text{Fiducial Time} \\ t_0 &\equiv \text{Start time of the exposure interval} \end{aligned}$$

The way in which the exposure time is selected results in an increase in the extent of the sky imaged over nominal field of view to $\approx 45^\circ$ along the X-direction and we have divided it in to 500 sky elements. The number of sky elements along the orthogonal Y direction depend on which mask pattern's shadow falls on which wire(s) (refer table 1.1) and 55 different mask-wire combinations can be listed. Thus the sky is modelled with 55 pixels along Y direction and 500 pixels along X direction.

In order to reconstruct the sky we perform a *derotation* in the sky plane using the recorded time of detection of the photons in order to correct for the rotation of the camera.

For every recorded photon in the event list and for each of the angles θ_f (corresponding to the sky elements) along the X direction at the fiducial time, a *derotation-angle* θ_d is calculated and the photon is *projected back* towards the sky plane through each of the six mask patterns. This is illustrated in figure 1.2 for a (single) hypothetical mask pattern.

For a given angle θ_f (along X direction) at the fiducial time, the derotation angle, θ_d is calculated as:

$$\theta_d = \theta_f + \dot{\theta}_x \times (t_p - t_f)$$

where,

$$\begin{aligned} \theta_d &\equiv \text{Derotation-angle, deg} \\ \theta_f &\equiv \text{Angle along the X-direction at the fiducial time, deg} \\ t_p &\equiv \text{Photon Strike Time, s} \end{aligned}$$

If the photons are projected (back) at an angle of θ_d , they will strike the mask plate at,

$$x_m = x_d - h \times \tan(\theta_d)$$

where,

$$\begin{aligned} x_m &\equiv \text{Mask plate strike position, mm} \\ x_d &\equiv \text{Detector wire strike position (from the event list), mm} \\ \theta_d &\equiv \text{Derotation-angle, deg} \end{aligned}$$

If this photon hits an open mask area of a pattern (that is when the calculated mask plate strike position, x_m is in an open mask area), the photon is added to the source contribution at the corresponding

m	COMBINATION
0	$W_8 P_1$
1	$W_8 P_1 + W_7 P_1$
2	$W_8 P_1 + W_7 P_1 + W_6 P_1$
3	$W_8 P_1 + W_7 P_1 + W_6 P_1 + W_5 P_1$
4	$W_8 P_1 + W_7 P_1 + W_6 P_1 + W_5 P_1 + W_4 P_1$
5	$W_8 P_1 + W_7 P_1 + W_6 P_1 + W_5 P_1 + W_4 P_1 + W_3 P_1$
6	$W_8 P_1 + W_7 P_1 + W_6 P_1 + W_5 P_1 + W_4 P_1 + W_3 P_1 + W_2 P_1$
7	$W_8 P_1 + W_7 P_1 + W_6 P_1 + W_5 P_1 + W_4 P_1 + W_3 P_1 + W_2 P_1 + W_1 P_1$
8	$W_8 P_2 + W_7 P_2 + W_6 P_2 + W_5 P_2 + W_4 P_2 + W_3 P_2 + W_2 P_2 + W_1 P_2$
9	$W_8 P_2 + W_7 P_2 + W_6 P_2 + W_5 P_2 + W_4 P_2 + W_3 P_2 + W_2 P_2 + W_1 P_2$
10	$W_8 P_2 + W_7 P_2 + W_6 P_2 + W_5 P_2 + W_4 P_2 + W_3 P_2 + W_2 P_2 + W_1 P_2$
11	$W_8 P_2 + W_7 P_2 + W_6 P_2 + W_5 P_2 + W_4 P_2 + W_3 P_2 + W_2 P_2 + W_1 P_2$
12	$W_8 P_2 + W_7 P_2 + W_6 P_2 + W_5 P_2 + W_4 P_2 + W_3 P_2 + W_2 P_2 + W_1 P_2$
13	$W_8 P_2 + W_7 P_2 + W_6 P_2 + W_5 P_2 + W_4 P_2 + W_3 P_2 + W_2 P_2 + W_1 P_2$
14	$W_8 P_2 + W_7 P_2 + W_6 P_2 + W_5 P_2 + W_4 P_2 + W_3 P_2 + W_2 P_2 + W_1 P_2$
15	$W_8 P_2 + W_7 P_2 + W_6 P_2 + W_5 P_2 + W_4 P_2 + W_3 P_2 + W_2 P_2 + W_1 P_2$
16	$W_8 P_2 + W_7 P_2 + W_6 P_2 + W_5 P_2 + W_4 P_2 + W_3 P_2 + W_2 P_2 + W_1 P_2$
17	$W_8 P_2 + W_7 P_2 + W_6 P_2 + W_5 P_2 + W_4 P_2 + W_3 P_2 + W_2 P_2 + W_1 P_2$
18	$W_8 P_2 + W_7 P_2 + W_6 P_2 + W_5 P_2 + W_4 P_2 + W_3 P_2 + W_2 P_2 + W_1 P_2$
19	$W_8 P_2 + W_7 P_2 + W_6 P_2 + W_5 P_2 + W_4 P_2 + W_3 P_2 + W_2 P_2 + W_1 P_2$
20	$W_8 P_2 + W_7 P_2 + W_6 P_2 + W_5 P_2 + W_4 P_2 + W_3 P_2 + W_2 P_2 + W_1 P_2$
21	$W_8 P_2 + W_7 P_2 + W_6 P_2 + W_5 P_2 + W_4 P_2 + W_3 P_2 + W_2 P_2 + W_1 P_2$
22	$W_8 P_2 + W_7 P_2 + W_6 P_2 + W_5 P_2 + W_4 P_2 + W_3 P_2 + W_2 P_2 + W_1 P_2$
23	$W_8 P_2 + W_7 P_2 + W_6 P_2 + W_5 P_2 + W_4 P_2 + W_3 P_2 + W_2 P_2 + W_1 P_2$
24	$W_8 P_2 + W_7 P_2 + W_6 P_2 + W_5 P_2 + W_4 P_2 + W_3 P_2 + W_2 P_2 + W_1 P_2$
25	$W_8 P_3 + W_7 P_3 + W_6 P_3 + W_5 P_3 + W_4 P_3 + W_3 P_3 + W_2 P_3 + W_1 P_3$
26	$W_8 P_3 + W_7 P_3 + W_6 P_3 + W_5 P_3 + W_4 P_3 + W_3 P_3 + W_2 P_3 + W_1 P_3$
27	$W_8 P_3 + W_7 P_3 + W_6 P_3 + W_5 P_3 + W_4 P_3 + W_3 P_3 + W_2 P_3 + W_1 P_3$
28	$W_8 P_3 + W_7 P_3 + W_6 P_3 + W_5 P_3 + W_4 P_3 + W_3 P_3 + W_2 P_3 + W_1 P_3$
29	$W_8 P_3 + W_7 P_3 + W_6 P_3 + W_5 P_3 + W_4 P_3 + W_3 P_3 + W_2 P_3 + W_1 P_3$
30	$W_8 P_3 + W_7 P_3 + W_6 P_3 + W_5 P_3 + W_4 P_3 + W_3 P_3 + W_2 P_3 + W_1 P_3$
31	$W_8 P_3 + W_7 P_3 + W_6 P_3 + W_5 P_3 + W_4 P_3 + W_3 P_3 + W_2 P_3 + W_1 P_3$
32	$W_8 P_3 + W_7 P_3 + W_6 P_3 + W_5 P_3 + W_4 P_3 + W_3 P_3 + W_2 P_3 + W_1 P_3$
33	$W_8 P_3 + W_7 P_3 + W_6 P_3 + W_5 P_3 + W_4 P_3 + W_3 P_3 + W_2 P_3 + W_1 P_3$
34	$W_8 P_3 + W_7 P_3 + W_6 P_3 + W_5 P_3 + W_4 P_3 + W_3 P_3 + W_2 P_3 + W_1 P_3$
35	$W_8 P_3 + W_7 P_3 + W_6 P_3 + W_5 P_3 + W_4 P_3 + W_3 P_3 + W_2 P_3 + W_1 P_3$
36	$W_8 P_3 + W_7 P_3 + W_6 P_3 + W_5 P_3 + W_4 P_3 + W_3 P_3 + W_2 P_3 + W_1 P_3$
37	$W_8 P_3 + W_7 P_3 + W_6 P_3 + W_5 P_3 + W_4 P_3 + W_3 P_3 + W_2 P_3 + W_1 P_3$
38	$W_8 P_3 + W_7 P_3 + W_6 P_3 + W_5 P_3 + W_4 P_3 + W_3 P_3 + W_2 P_3 + W_1 P_3$
39	$W_8 P_3 + W_7 P_3 + W_6 P_3 + W_5 P_3 + W_4 P_3 + W_3 P_3 + W_2 P_3 + W_1 P_3$
40	$W_8 P_3 + W_7 P_3 + W_6 P_3 + W_5 P_3 + W_4 P_3 + W_3 P_3 + W_2 P_3 + W_1 P_3$
41	$W_8 P_3 + W_7 P_3 + W_6 P_3 + W_5 P_3 + W_4 P_3 + W_3 P_3 + W_2 P_3 + W_1 P_3$
42	$W_8 P_3 + W_7 P_3 + W_6 P_3 + W_5 P_3 + W_4 P_3 + W_3 P_3 + W_2 P_3 + W_1 P_3$
43	$W_8 P_3 + W_7 P_3 + W_6 P_3 + W_5 P_3 + W_4 P_3 + W_3 P_3 + W_2 P_3 + W_1 P_3$
44	$W_8 P_3 + W_7 P_3 + W_6 P_3 + W_5 P_3 + W_4 P_3 + W_3 P_3 + W_2 P_3 + W_1 P_3$
45	$W_8 P_3 + W_7 P_3 + W_6 P_3 + W_5 P_3 + W_4 P_3 + W_3 P_3 + W_2 P_3 + W_1 P_3$
46	$W_8 P_3 + W_7 P_3 + W_6 P_3 + W_5 P_3 + W_4 P_3 + W_3 P_3 + W_2 P_3 + W_1 P_3$
47	$W_8 P_3 + W_7 P_3 + W_6 P_3 + W_5 P_3 + W_4 P_3 + W_3 P_3 + W_2 P_3 + W_1 P_3$
48	$W_7 P_6 + W_6 P_6 + W_5 P_6 + W_4 P_6 + W_3 P_6 + W_2 P_6 + W_1 P_6$
49	$W_6 P_6 + W_5 P_6 + W_4 P_6 + W_3 P_6 + W_2 P_6 + W_1 P_6$
50	$W_5 P_6 + W_4 P_6 + W_3 P_6 + W_2 P_6 + W_1 P_6$
51	$W_4 P_6 + W_3 P_6 + W_2 P_6 + W_1 P_6$
52	$W_3 P_6 + W_2 P_6 + W_1 P_6$
53	$W_2 P_6 + W_1 P_6$
54	$W_1 P_6$

Table 1.1: First column lists the sky element number (m) along Y direction and the second column specifies the corresponding mask-wire combination. $W_a P_b \Rightarrow$ 1-d sky image due to (back) projection of photons recorded on Wire number a towards mask pattern number b , \forall ($1 \leq a \leq 8$) & ($1 \leq b \leq 6$)

θ_f in the (1-d) sky image due to that *Wire-Pattern* combination, otherwise (if the photon hits a closed mask area), the photon is added to the background contribution at that θ_f in the *Wire-Pattern* sky image. The *Wire* in the *Wire-Pattern* combination is the one on which the photon was recorded, as per the event list and the *Pattern* is the mask pattern towards which the photon was projected (back).

After this procedure is employed on all the recorded photons, at every angle along X-direction (θ_f) at the fiducial time, in each of the 48 1-d *Wire-Pattern* sky images (48 because there are 8 wires and 6 mask patterns in a camera), the total background contribution is subtracted from the total source contribution and the resultant is stored as the photon-count contribution at that sky element corresponding to some θ_f .

The 48 1-d images are coadded based on the 55 Wire-Mask combinations of table 1.1 to obtain the raw reconstructed image of 55×500 pixels.

Some of the results of back-projection reconstruction are shown in figures 1.3, 1.4, and 1.5. Each of these cases have been simulated with the camera rotated along the X-direction at a rate of $\frac{1}{15}^\circ/s$ (and not rotated along the Y-direction). The source locations and the values of σ_x and σ_y used are mentioned in the captions of the figures.

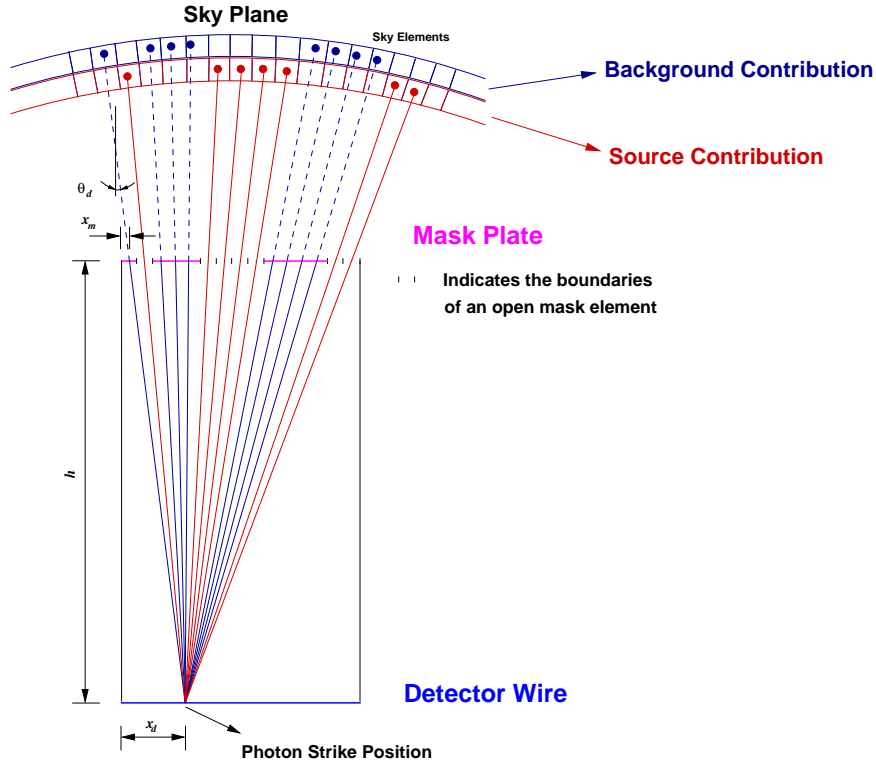


Figure 1.2: Back-Projecting the recorded photon strike position in the Derotation direction

1.3 Iterative Removal Of Sources

The procedure of Iterative Removal Of Sources (IROS) is employed on the raw reconstructed sky image (obtained by back-projection reconstruction) in order to find the locations and fluxes of the sources and to distinguish source peaks from those produced due to coding noise, and hence improve the dynamic range of the image. The response of the camera for sources at different sky elements will be unique and are known (Point Spread Functions, PSFs). The IROS is essentially a PSF-removal procedure.

1.3.1 PSF-generation

The PSFs are generated by simulating a source at each of the sky elements at a time, and then normalising the raw reconstructed image (obtained after the back-projection) for unit flux.

The procedure for simulation is almost same as that explained in page 1 excepting for a few changes. In order to reduce the Poisson Noise, the number of photons to be detected is specified as a large number (and flux of the source is not specified from which the number of photons to be generated used to be calculated as in the other procedure explained in page 1). A value of 10^6 has been used for the number of photons to be detected. The photons are generated only for the duration for which the source will be present in the nominal field of view (FOV).

For a given source, the value of the time interval between the photons to be generated is calculated as:

$$t_i = \frac{t_s}{n_d} \times \frac{a_m}{2 \times a_s}$$

where,

t_i	\equiv	Time Interval between the photons to be generated, s
t_s	\equiv	Time Duration for which the source will be in the nominal FOV, s
n_d	\equiv	Number of photons to be detected ($=10^6$)
a_m	\equiv	Maximum Effective Open Mask area relevant for the specified source, mm^2
a_s	\equiv	Total Effective Mask area relevant for the specified source, mm^2

NOTE:

1. The term *effective* here refers to the area of the mask plate whose shadow falls on the detector.
- 2 The factor 2 is used (in the equation) to consider the average of the Maximum Effective Open Mask Area: $\frac{a_m}{2}$, as the effective area of the mask keeps changing due to the rotation.

The camera is rotated only along the X-direction (at a rate of $\frac{1}{15}^\circ/\text{s}$). Using the event list generated, the back-projection reconstruction is undertaken and the photon-counts at every pixel in the resulting raw image is multiplied by the following factor, to normalise them for unit flux ($1 \text{ cnt cm}^2 \text{ s}$):

$$s = \frac{t_s \times a_t}{n_g}$$

where,

s	\equiv	Scaling factor to be used with the photon-counts at every pixel of the raw reconstructed image, $1 \text{ cnt cm}^2 \text{ s}$
t_s	\equiv	Time Duration for which the source specified (for which the PSF has to be generated) is within the nominal FOV, s
a_t	\equiv	Total Mask Plate Area, cm^2
n_g	\equiv	Number of photons generated during the simulation for the source specified

1.3.2 The procedure of IROS

At every step of iteration of the IROS, the RMS-reduction resulting due to the removal of responses due to candidate peaks picked from the reconstructed sky image are noted down and the candidate which gives the largest reduction in the image RMS is selected as the valid source. The criterion for picking the candidates is just the peak-strength in the reconstructed image. The first candidate will be the strongest peak in the image. Looking for candidates is stopped once a picked candidate does not reduce the RMS beyond a specified limit. The response due to the selected source is modelled and removed from the reconstructed sky image. This is summarised in the equation below (supposing that a source has been found at (Sky-Element-Y, Sky-Element-X) = (m, k)):

$$I(i, j) = I(i, j) - \frac{I(m, k)}{P_{m,k}(m, k)} \times P_{m,k}(i, j) \quad \forall \quad 0 \leq i \leq 54, \quad 0 \leq j \leq 499$$

where,

i	\equiv	Sky Element along Y-direction
j	\equiv	Sky Element along X-direction
I	\equiv	Sky Image from which the modelled response has to be removed
$P_{m,k}$	\equiv	PSF at (m, k) at which the source is located.

In the next step of iteration, new candidates are looked for from the residual map remaining after the removal of a *valid* source in the previous iteration. The usual RMS improvement criterion is applied, but if some residual (either positive or negative) has cropped up in any of the *already declared* source locations, it is modelled and removed irrespective of the RMS criterion. The iteration is stopped when, either there is **no** candidate left in the image which can reduce the RMS value beyond the specified limit, or if at all there are candidate peaks, all of them are *first-time-negative-peaks*. The residuals removed from source locations are added to their respective source-fluxes and a consolidated list of sources is generated at the end. The residual image obtained at the end of the IROS will mainly be due to the Poisson noise, which cannot be modelled and removed. The consolidated source strengths are added to the residual image at their respective locations. A table listing the flux values (in the units of $\text{cnts cm}^{-2} \text{ s}^{-1}$) for the sources picked is also generated.

The results of processing the raw reconstructed images shown in figures 1.3, 1.4 and 1.5 through IROS are shown in figures 1.6, 1.7 and 1.8 respectively.

The grid lines in the figures span the nominal FOV. As has already been mentioned the effective FOV is larger than the nominal FOV and we can reconstruct sources present outside the nominal FOV. This is illustrated in example set 2 (figures 1.4 and 1.7) in which one of the sources: at $(Y,X)=(37.00^\circ, 13.35^\circ)$ and of input flux 850 mCrab, is present outside the nominal FOV.

The example 3 (figures 1.5 and 1.8) is used to illustrate the dynamic range. No impressions of the weaker source of input flux 250 mCrab present at $(Y,X)=(22.62^\circ, 8.19^\circ)$ can be seen in the raw image in figure 1.5 as the coding noise due to the 1 Crab source elsewhere in the FOV is dominant. It has been possible to pick the weaker source during the IROS and also reconstruct its flux to a good accuracy (when compared to the input flux).

1.4 Noise Characteristics

We try to obtain the systematic pattern in the sky image generated by the back-projection reconstruction technique for a pure noise input. We intend to use this as a noise model during the IROS procedure.

A total of 220 background noise simulations have been done. Monte Carlo methods have been used for the simulation during which noise photons are randomly placed on the detector plane using random number generator (which follows a uniform distribution). Every simulation has been carried out with different random-seeds (used to initialise the random number generator) for a time duration of t_e s (exposure time, page 1) and with a background count rate of 80 cts s^{-1} , which results in 27143 noise photons per simulation, for $t_e = 339.297805$ s.

A back-projection reconstruction (page 2) is undertaken for all of the 220 noise simulations. An average of all the back-projection images (here after referred to as grand average image) has been obtained (figure 1.9). The Poisson Noise level in the grand average image will be much lower than that in the individual noise-images. To check the fidelity of the grand average image, we obtained an image by having a regular grid data, placed uniformly in both space and time. This image will not have any Poisson Noise but a systematic wavy pattern having six peaks across the mask coding direction and a collimator response along the mask coding direction (figure 1.10). We obtained a difference image by subtracting the grand average image (figure 1.9) from the back-projection image obtained by having a regular grid data (figure 1.10). In this difference image shown in figure 1.11 the wavy pattern across the coding direction is clearly seen.

The grand average image has been normalised (to the units of per noise-photon) by a factor: 27143 which is the number of photons in each of the 220 noise simulations. The normalised image shown in figure 1.12 will be used as the noise characteristic of the back-projection reconstruction technique. During the procedure of IROS, this noise characteristic can be scaled to the required noise level to check the validity of sources picked. That is, if a source picked at any sky pixel happens to be below the scaled noise-level at the same pixel in the noise-characteristic image, the source is discarded, assuming it to be a false alarm.

Further, a set of 10 images each of which is an average of 20 back-projection images (picked from the 220 reconstructed images) have been obtained. Each averaged-image in the set of 10 is subtracted from the (unnormalised) grand average image and these difference images have been analysed. The difference images are dominated by the random Poisson Noise and so the systematic wavy-pattern is not seen very clearly. Figure 1.13 shows the wavy pattern in the image obtained by subtracting tenth set from the grand average image and figure 1.14 shows the collimator response in the same difference image.

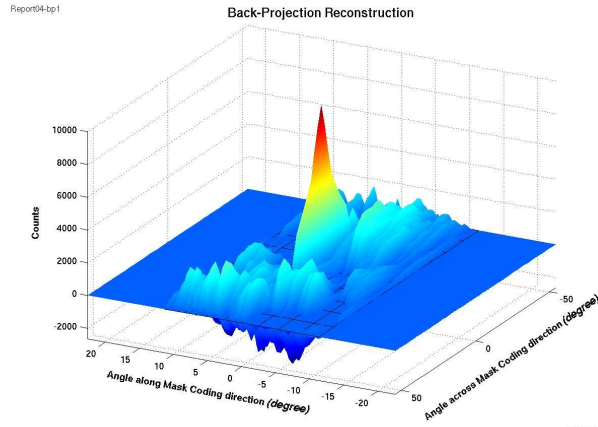


Figure 1.3: $\sigma_x=0.5$ mm, $\sigma_y=3.0$ mm,
 Src: (Y,X)=(0.00°,0.05°), Input Flux=1.00 Crab

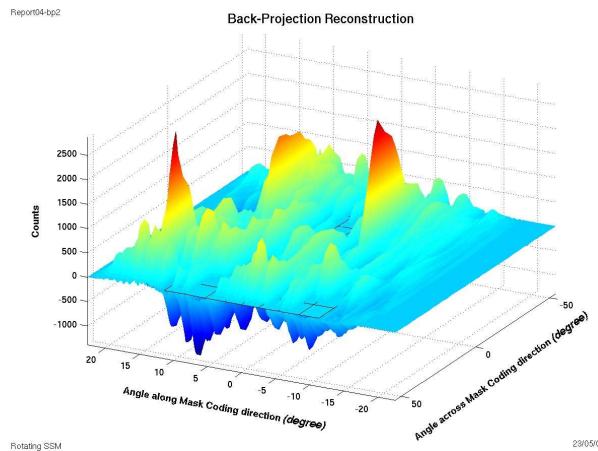


Figure 1.4: $\sigma_x=0.5$ mm, $\sigma_y=3.0$ mm,
 Src1: (Y,X)=(37.00°,13.35°), Input Flux=0.85 Crab
 Src2: (Y,X)=(-6.84°, -6.74°), Input Flux=0.30 Crab

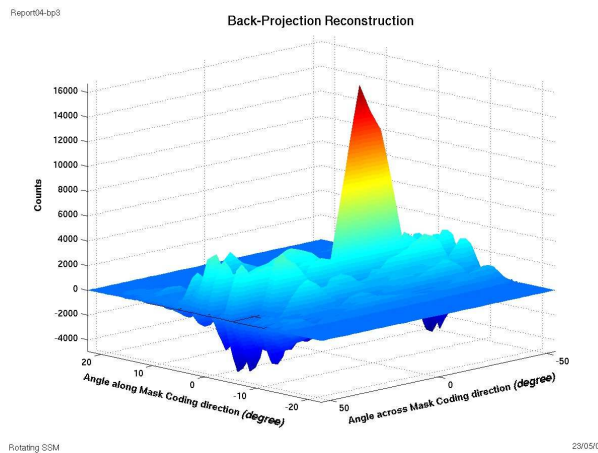


Figure 1.5: $\sigma_x=0.0$ mm, $\sigma_y=0.0$ mm,
 Src1: (Y,X)=(-6.84°, -4.48°), Input Flux=1.00 Crab
 Src2: (Y,X)=(22.62°,8.19°), Input Flux=0.25 Crab

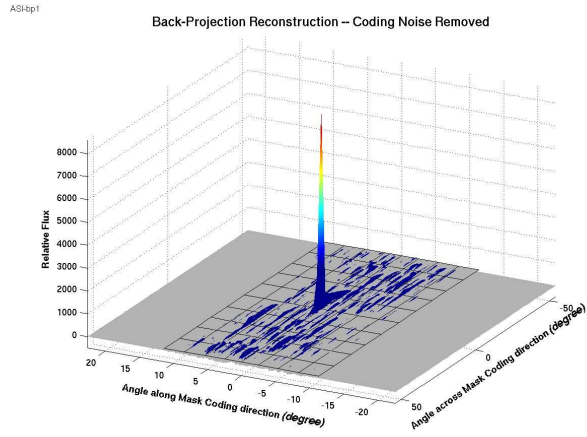


Figure 1.6: $\sigma_x=0.5$ mm, $\sigma_y=3.0$ mm,
 Src: (Y,X)=(0.00°,0.05°), Reconstructed Flux= 3.40 cnts cm⁻² s⁻¹ (0.95 Crab)

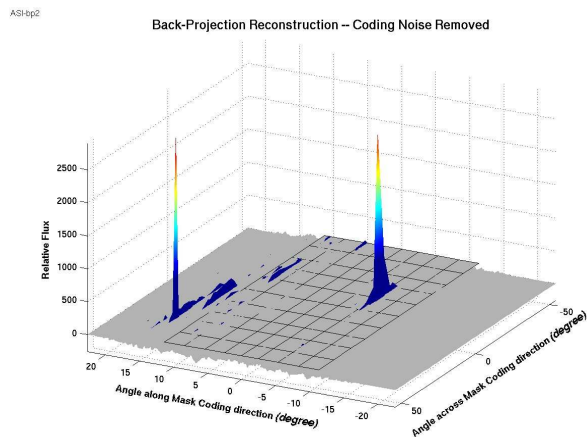


Figure 1.7: $\sigma_x=0.5$ mm, $\sigma_y=3.0$ mm,
 Src1: (Y,X)=(37.00°,13.35°), Reconstructed Flux= 2.89 cnts cm⁻² s⁻¹ (0.81 Crab)
 Src2: (Y,X)=(-6.84°,-6.74°), Reconstructed Flux= 0.81 cnts cm⁻² s⁻¹ (0.23 Crab)

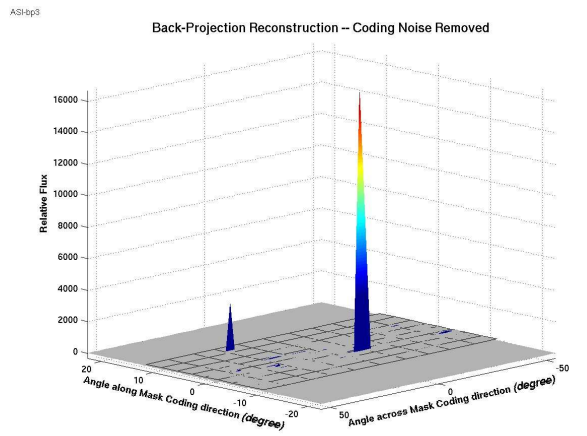


Figure 1.8: $\sigma_x=0.0$ mm, $\sigma_y=0.0$ mm,
 Src1: (Y,X)=(-6.84°,-4.48°), Reconstructed Flux= 3.57 cnts cm⁻² s⁻¹ (1 Crab)
 Src2: (Y,X)=(22.62°,8.19°), Reconstructed Flux= 0.88 cnts cm⁻² s⁻¹ (0.24 Crab)

Grand Average of the 220 Back-Projection Images

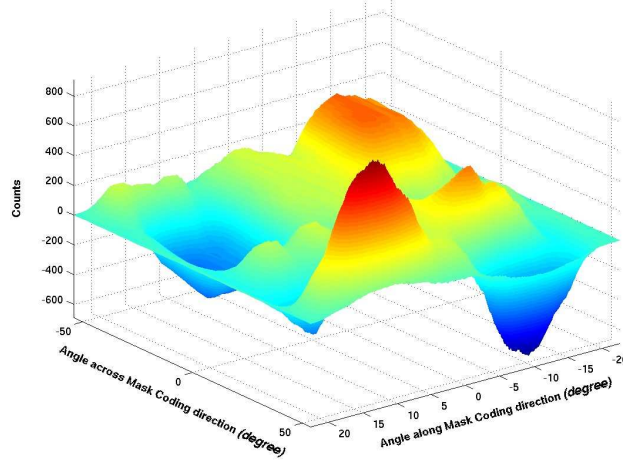


Figure 1.9: Grand Average Image

Back-Projection Image obtained using regular-grid data

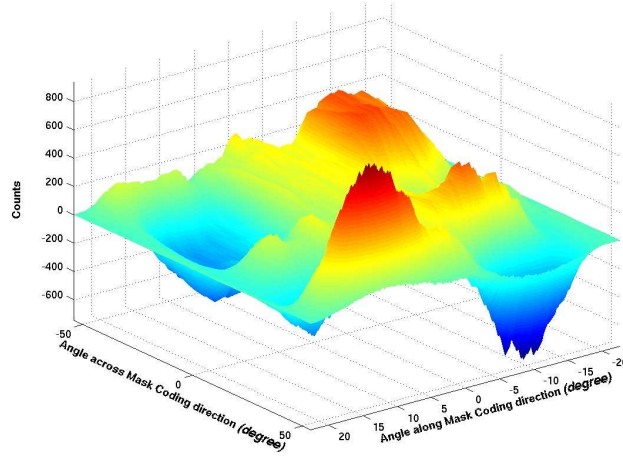


Figure 1.10: Back-Projection Image using a regular grid data

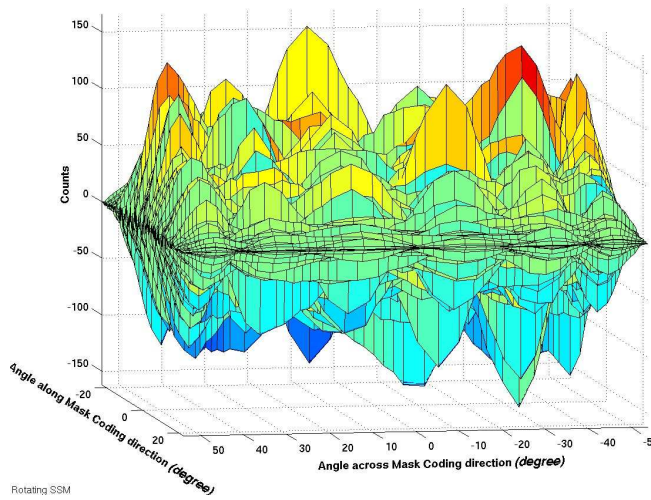


Figure 1.11: The grand average image subtracted from the image using a regular grid data

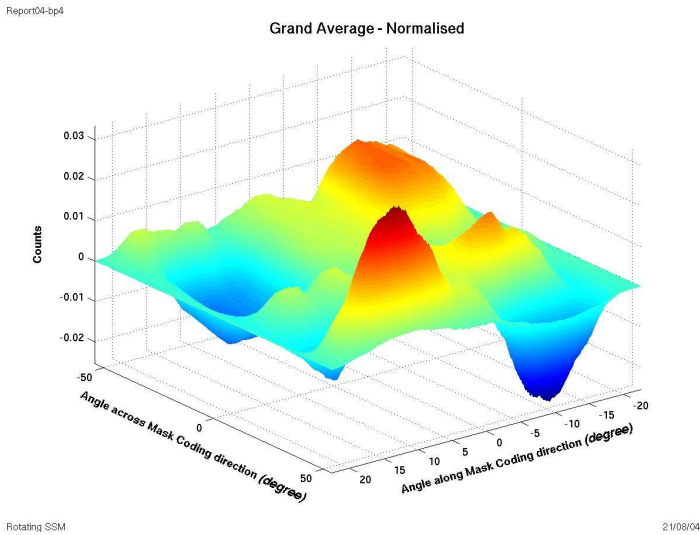


Figure 1.12: Noise Characteristic

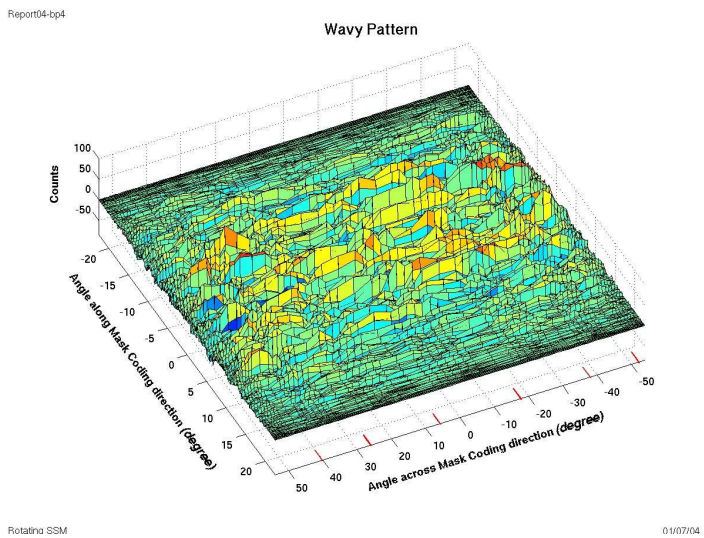


Figure 1.13: Grand Average Image minus Image of Set-10. The wavy pattern across the mask coding direction. The positions of the six peaks in the wavy pattern are indicated by the tic-marks towards the inside of the axis representing the cross-coding direction

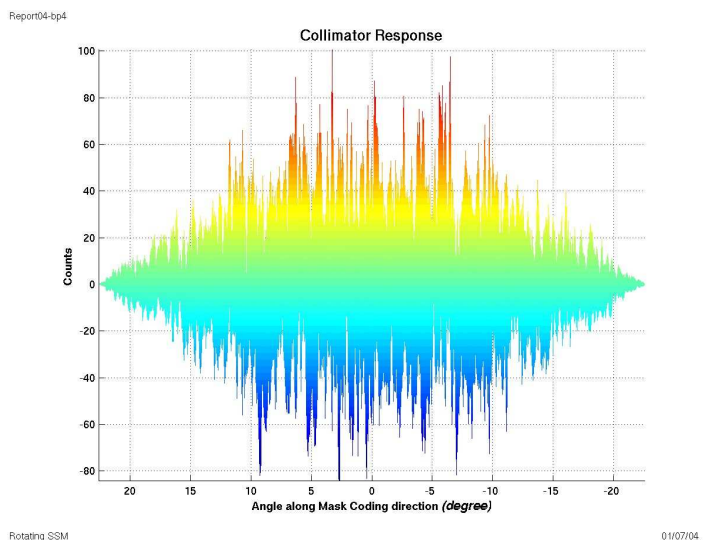


Figure 1.14: Grand Average Image minus Image of Set-10. Collimator response along the mask coding direction